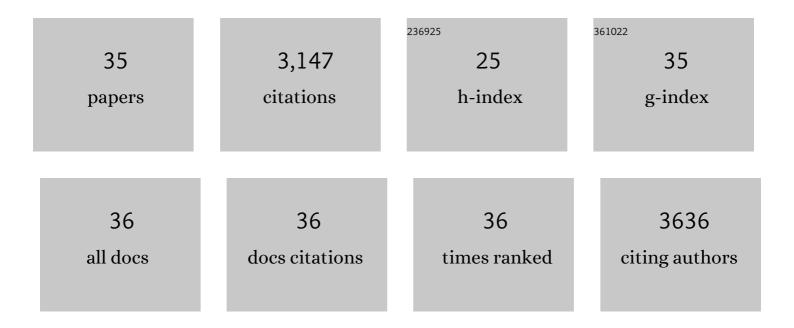
Xing Ding

List of Publications by Year in descending order

Source: https://exaly.com/author-pdf/7193862/publications.pdf Version: 2024-02-01



#	Article	IF	CITATIONS
1	Superoxide anion and singlet oxygen dominated faster photocatalytic elimination of nitric oxide over defective bismuth molybdates heterojunctions. Journal of Colloid and Interface Science, 2022, 618, 248-258.	9.4	4
2	Insights into the Surface/Interface Modifications of Bi ₂ MoO ₆ : Feasible Strategies and Photocatalytic Applications. Solar Rrl, 2021, 5, 2000442.	5.8	29
3	Chloridion-induced dual tunable fabrication of oxygen-deficient Bi2WO6 atomic layers for deep oxidation of NO. Chinese Journal of Catalysis, 2021, 42, 1013-1023.	14.0	17
4	Continuously tuning the hydrogen evolution activity of MoS2 through sodium ions insertion. Electrochimica Acta, 2021, 369, 137686.	5.2	1
5	Insight into surface hydroxyl groups for environmental purification: characterizations, applications and advances. Surfaces and Interfaces, 2021, 25, 101272.	3.0	7
6	Deep insight into ROS mediated direct and hydroxylated dichlorination process for efficient photocatalytic sodium pentachlorophenate mineralization. Applied Catalysis B: Environmental, 2021, 296, 120352.	20.2	42
7	Insight into the effect of bromine on facet-dependent surface oxygen vacancies construction and stabilization of Bi2MoO6 for efficient photocatalytic NO removal. Applied Catalysis B: Environmental, 2020, 265, 118585.	20.2	96
8	Highly Intensified Molecular Oxygen Activation on Bi@Bi ₂ MoO ₆ via a Metallic Bi-Coordinated Facet-Dependent Effect. ACS Applied Materials & Interfaces, 2020, 12, 1867-1876.	8.0	54
9	lodine-doping-assisted tunable introduction of oxygen vacancies on bismuth tungstate photocatalysts for highly efficient molecular oxygen activation and pentachlorophenol mineralization. Chinese Journal of Catalysis, 2020, 41, 1544-1553.	14.0	17
10	Constructing electron delocalization channels in covalent organic frameworks powering CO2 photoreduction in water. Applied Catalysis B: Environmental, 2020, 274, 119096.	20.2	113
11	Targeted removal of interfacial adventitious carbon towards directional charge delivery to isolated metal sites for efficient photocatalytic H2 production. Nano Energy, 2020, 76, 105077.	16.0	24
12	Intermolecular cascaded π-conjugation channels for electron delivery powering CO2 photoreduction. Nature Communications, 2020, 11, 1149.	12.8	147
13	Oxygen vacancies induced special CO2 adsorption modes on Bi2MoO6 for highly selective conversion to CH4. Applied Catalysis B: Environmental, 2019, 259, 118088.	20.2	221
14	Controlling Monomer Feeding Rate to Achieve Highly Crystalline Covalent Triazine Frameworks. Advanced Materials, 2019, 31, e1807865.	21.0	158
15	Oxygen vacancy boosted photocatalytic decomposition of ciprofloxacin over Bi2MoO6: Oxygen vacancy engineering, biotoxicity evaluation and mechanism study. Journal of Hazardous Materials, 2019, 364, 691-699.	12.4	226
16	Molecular structure design of conjugated microporous poly(dibenzo[b,d]thiophene 5,5-dioxide) for optimized photocatalytic NO removal. Journal of Catalysis, 2018, 357, 188-194.	6.2	25
17	Conjugated Polymers with Sequential Fluorination for Enhanced Photocatalytic H ₂ Evolution via Proton-Coupled Electron Transfer. ACS Energy Letters, 2018, 3, 2544-2549.	17.4	109
18	Simple fabrication of Fe ₃ O ₄ /C/g-C ₃ N ₄ two-dimensional composite by hydrothermal carbonization approach with enhanced photocatalytic performance under visible light. Catalysis Science and Technology, 2018, 8, 3484-3492.	4.1	32

XING DING

#	Article	IF	CITATIONS
19	Pyrene-Based Conjugated Polymer/Bi2MoO6 Z-Scheme Hybrids: Facile Construction and Sustainable Enhanced Photocatalytic Performance in Ciprofloxacin and Cr(VI) Removal under Visible Light Irradiation. Catalysts, 2018, 8, 185.	3.5	9
20	Fe@Fe 2 O 3 promoted electrochemical mineralization of atrazine via a triazinon ring opening mechanism. Water Research, 2017, 112, 9-18.	11.3	84
21	Synthesis of 1,4-diethynylbenzene-based conjugated polymer photocatalysts and their enhanced visible/near-infrared-light-driven hydrogen production activity. Journal of Catalysis, 2017, 350, 64-71.	6.2	85
22	Highly efficient visible light induced photocatalytic activity of a novel in situ synthesized conjugated microporous poly(benzothiadiazole)–C ₃ N ₄ composite. Catalysis Science and Technology, 2017, 7, 418-426.	4.1	30
23	Lightâ€5witchable Oxygen Vacancies in Ultrafine Bi ₅ O ₇ Br Nanotubes for Boosting Solarâ€Driven Nitrogen Fixation in Pure Water. Advanced Materials, 2017, 29, 1701774.	21.0	533
24	Surface plasmon resonance-induced visible-light photocatalytic performance of silver/silver molybdate composites. Chinese Journal of Catalysis, 2017, 38, 260-269.	14.0	31
25	Novel in situ fabrication of conjugated microporous poly(benzothiadiazole)–Bi2MoO6 Z-scheme heterojunction with enhanced visible light photocatalytic activity. Journal of Catalysis, 2017, 345, 319-328.	6.2	71
26	In Situ Carbon Homogeneous Doping on Ultrathin Bismuth Molybdate: A Dualâ€Purpose Strategy for Efficient Molecular Oxygen Activation. Advanced Functional Materials, 2017, 27, 1703923.	14.9	136
27	Photocatalysis: Lightâ€5witchable Oxygen Vacancies in Ultrafine Bi ₅ O ₇ Br Nanotubes for Boosting Solarâ€Driven Nitrogen Fixation in Pure Water (Adv. Mater. 31/2017). Advanced Materials, 2017, 29, .	21.0	2
28	Conjugated microporous poly(benzothiadiazole)/TiO2 heterojunction for visible-light-driven H2 production and pollutant removal. Applied Catalysis B: Environmental, 2017, 203, 563-571.	20.2	94
29	A plate-on-plate sandwiched Z-scheme heterojunction photocatalyst: BiOBr-Bi 2 MoO 6 with enhanced photocatalytic performance. Applied Surface Science, 2017, 391, 194-201.	6.1	238
30	Self doping promoted photocatalytic removal of no under visible light with bi2moo6: Indispensable role of superoxide ions. Applied Catalysis B: Environmental, 2016, 182, 316-325.	20.2	157
31	A dual-cell wastewater treatment system with combining anodic visible light driven photoelectro-catalytic oxidation and cathodic electro-Fenton oxidation. Separation and Purification Technology, 2014, 125, 103-110.	7.9	25
32	Enhanced Photocatalytic Removal of Sodium Pentachlorophenate with Self-Doped Bi ₂ WO ₆ under Visible Light by Generating More Superoxide lons. Environmental Science & Technology, 2014, 48, 5823-5831.	10.0	239
33	Design of a visible light driven photo-electrochemical/electro-Fenton coupling oxidation system for wastewater treatment. Journal of Hazardous Materials, 2012, 239-240, 233-240.	12.4	29
34	Efficient visible light driven photocatalytic removal of NO with aerosol flow synthesized B, N-codoped TiO2 hollow spheres. Journal of Hazardous Materials, 2011, 190, 604-612.	12.4	58
35	H ₃ BO ₃ -Induced Formation of Metal Oxide Hollow Spheres in Flowing Aerosols. Journal of Physical Chemistry C, 2009, 113, 5455-5459.	3.1	4